ACTA IMEKO
ISSN: 2221-870X
September 2024, Volume 13, Number 3, 1 - 6

Green synthesis and characterization of titanium dioxide nanoparticles and their photocatalytic activity

Eleonora Marconi[1,2], Igor Luisetto[3], Luca Tortora[1,4]

[1] *Istituto Nazionale di Fisica Nucleare INFN, sezione Roma Tre, via della Vasca Navale 84, Rome, 00146, Italy*
[2] *Centro di Eccellenza DTC Lazio, c/o Palazzo del Rettorato Sapienza Università di Roma Piazzale Aldo Moro 5, Rome 00185, Italy*
[3] *Dipartimento Tecnologie Energetiche e Fonti Rinnovabili, ENEA centro di ricerche, Casaccia, Via Anguillarese 301, 00123 Rome, Italy*
[4] *Dipartimento di Scienze, Università Roma Tre, via della Vasca Navale 84, Roma, 00146, Italy*

ABSTRACT
In this study, we compared two low-temperature synthesis procedures for the large-scale production of titania nanoparticles (NPs). The first takes place in an aqueous medium with an acidic environment, by using a triblock polymer surfactant (Pluronic 123). The second involves a polycondensation reaction of alkoxide precursors at 70 °C in a water-in-oil (W/O) microemulsion with a volume ratio of 1:1, using cetylpyridinium bromide (CPB) as a cationic surfactant. The morphological and structural characterization of the samples was carried out through Scanning Electron Microscopy (SEM) and X-Ray Diffraction (XRD). The photoactivity of the nanostructured titania was evaluated by measuring the photodegradation of Methylene Blue (MB). The solvent-free synthetic approach provided spherical titania nanoparticles mainly constituted by rutile crystallites with a very good synthetic yield. However, the photodegradation rate of MB for such titania nanoparticles ranges from 30 % to 40 %, after 1h under solar irradiation. Conversely, titania nanoparticles obtained through microemulsion synthesis show a photodegradation rate of more than 90 % comparable to titania P25. This high-yield synthesis leads to the formation of TiO_2 nanoparticles characterized by small crystallite aggregates (rutile and anatase).

Section: RESEARCH PAPER

Keywords: titanium dioxide; microemulsion; templating synthesis; photocatalysis

Citation: E. Marconi, I. Luisetto, L. Tortora, Green synthesis and characterization of titanium dioxide nanoparticles and their photocatalytic activity, Acta IMEKO, vol. 13 (2024) no. 3, pp. 1-6. DOI: 10.21014/actaimeko.v13i3.1775

Section Editor: Fabio Leccese, Università Degli Studi Roma Tre, Rome, Italy

Received February 12, 2024; **In final form** June 7, 2024; **Published** September 2024

Corresponding author: Eleonora Marconi, e-mail: eleonora.marconi@roma3.infn.it

1. INTRODUCTION

Self-cleaning material became increasingly attractive since it can save time and maintenance costs [1]-[4]. New technologies are being developed around self-cleaning coating to apply on natural and artificial stone [5]. The issue of soiling of the building surface is so significant that in recent years a considerable effort has carried out on the development of policies for reducing atmospheric pollutants, not only to reduce human health risks but also to reduce the soiling of building materials [6]. However, the persistent presence of oil particulates and organic carbon continues to pose difficulties. An innovative strategy for addressing this issue involves the implementation of self-cleaning techniques using photocatalytic surfaces, that represents a promising avenue to prevent soiling and provide cleanliness [7]. Photocatalytic materials can oxidize contaminants and bio-organisms, thanks to the redox reactions that take place on their surface when electron/hole pairs, generated by light irradiation, migrate to the surface. Among photocatalytic materials, TiO_2 (in the mineral form of anatase and rutile) has been extensively studied and used because it has the most effective photoactivity, the highest stability, and the lowest cost among semiconductor metal oxides [8]. In newly constructed structures, the photocatalytic properties of TiO_2 have been harnessed by incorporating nanoparticles into paints [9], mortars, tiles [10], and glasses [11], thereby imparting self-cleaning, antimicrobial, smog-eating, and air-purifying functionalities. In the field of Cultural Heritage, TiO_2, with its "smog-eating" and self-cleaning coating capabilities, can find application [12], serving also as a biocide [13], [14]. Typically, TiO_2 nanoparticles are dispersed within a transparent polymeric film, creating an adhesive material and crack-free coatings suitable for protecting stone surfaces [15] and providing film protection for building walls. Furthermore, the application of titania nanoparticles in coating formulations results in a self-cleaning surface, attributed to the hydrophobic/hydrophilic ability activated by solar irradiation

[16], thereby preventing soiling and preserving cleanliness on architectural substrates.

In the last few years, commercial Degussa P25 TiO_2 nanoparticles became the reference point for photo-reactivity in applications involving environmental volatile organic compounds (VOC) [17]. Degussa P25 is characterized as a non-porous nanoparticle with a composition of 70 % anatase and 30 % rutile, featuring an anatase phase that exhibits better reactivity compared to pure rutile [18]. However, the fabrication method of the Degussa P25, the most diffused photocatalyst for application in architectural field, is protected by a patent and thus the synthesis approach is actually not fully available. In general, the prevalent industrial method for titanium dioxide production involves extracting TiO_2 from the ilmenite mineral. Ilmenite ($FeTiO_3$) constitutes approximately 92 % of the global consumption of titanium minerals, with nearly 95 % of these minerals dedicated to the production of TiO_2 pigment products [19], [20]. Several approaches have been investigated to mitigate the environmental impact associated with the production of titania nanoparticles, including chemical, physical, and biological synthesis methods [21], [22]. Among the different synthetic approaches, biological methods have gained strong interest in recent years. The concept of "green synthesis" is closely related to the biological methods; these are mainly based on two different approaches: (a) photosynthesis, where synthesis can be carried out through plants and their extracts, and (b) biosynthesis, which involves synthesis from extracts of bacteria, algae, fungi, and actinomycetes [23]. However, while the biological route dominates the green approach to synthesizing titania nanoparticles, the challenge lies in enhancing the efficiency of biological synthesis, particularly in scaling up for industrial applications [24].

Within the chemical synthesis methods, sol-gel, hydrothermal, and microemulsion techniques stand out as the most frequently utilized [25], [26]. Several factors can influence the synthesis of titania nanoparticles, including the choice of precursor (alkoxide or metal salt), the type of surfactant (ionic, non-ionic, triblock copolymer), and calcination temperature [27]. The selection of the titanium precursor can affect the hydrolysis and condensation reactions to the formation of the mesoporous network [28]. The employed surfactant impacts on the template spatial organization and therefore on the morphology of the titania nanoparticles [29], while calcination, required to eliminate organic residues, affects the polymorph type of TiO_2 and the size of the crystalline grains [30]. As reported in the literature, the microemulsion synthesis method offers a higher yield percentage of titania powder compared to other chemical processes. Specifically, the prevailing trend is microemulsion > sol-gel > solvothermal > hydrothermal, with respective synthesis yields of 85 %, 80 %, 78 %, and 75 % [24]. In general, the titania powder obtained through microemulsion synthesis shows a notable surface area (around 250 $m^2\ g^{-1}$) and crystallites with small size (50 nm) [31]. The microemulsion process stands out as an environmentally sustainable synthesis method when compared to alternative approaches. It demonstrates reduced greenhouse gas emissions in contrast to biological routes and minimizes the use of organic solvents typically associated with sol-gel and solvothermal processes [27]. However, the microemulsion process usually entails the use of a water-in-oil (W/O) system with high oil volume content. Therefore, the organic solvent still represents a significant portion of the synthesis process [32], [33]. In this study, we compared two synthesis protocols based on a microemulsion system with a W:O volume ratio of 1:1, operating under atmospheric pressure and low temperature, and a one-pot synthesis that is solvent-free followed by hydrothermal treatment. This study was also conceived with the crucial aim of identifying the most efficient synthesis route for producing titania nanoparticles through the innovative use of a solvent-free procedure. This research is driven by the imperative goal of enhancing the synthesis yield while maintaining a focus on facilitating industrial-scale production.

2. MATERIALS AND METHODS

2.1. Chemicals

Tetraethyl orthotitanate (TEOT), Titanium butoxide (TiBUT), cyclohexane, 1-penthanol, cetylpyridinium bromide (CPB), Pluronic 123 (P123), hydrochloric acid 37 % (v/v), methylene blue (MB), urea, and ultrapure water were purchased from Merck S.r.l. (Germany).

2.2. Microemulsion synthesis

Titania nanoparticles were obtained by microemulsion synthesis with the reflux method. The microemulsion consists of an oil phase, composed of 30.0 mL of cyclohexane and 1.5 mL 1-pentanol droplet into the aqueous phase, composed of 30.0 mL water, 1.0 g CPB, and 0.6 g urea. The mixture was vigorously stirred for 1 hour. After that, 10.0 mmol of titanium precursor was added to the microemulsion obtained. The mixture was stirred at room temperature for 1 h, then refluxed for 48 h at 70 °C. The powder was collected by centrifuge, washed several times in water and ethanol, dried, and finally calcined at 450 or 600 °C for 4 h [34].

2.3. One-pot synthesis

Titania nanoparticles were obtained by one-pot synthesis and subsequent hydrothermal treatment. First, 1.0 g of P123 was dissolved in 30.0 mL of distilled water and 5.7 mL of hydrochloric acid 37 wt %. Next, 7.0 mmol of titanium precursor was added to the aqueous solution under vigorous stirring for 24 hours at 40 °C. The aqueous solution was then put in the hydrothermal reactor for 24 hours at 100 °C. The powder obtained was collected by centrifuge, washed several times with water and ethanol, dried, and calcined at 450 °C for 4 hours. Table 1 summarizes all samples obtained [35].

2.4. Characterization

Morphological and textural properties of titania nanoparticles were studied under the Scanning Electron Microscope (FE-SEM ZEISS SIGMA 300, Germany). The samples were observed at a high vacuum with an accelerating voltage of 10 kV. Crystallographic phase and crystallite size were determined using a SCINTAG diffractometer (San Francisco, USA) within the 2θ range of 2-70 ° at a rate of 3 min^{-1}. All the measurements were carried out at room temperature using Cu Kα radiation (λ = 1.54 Å). The Scherrer equation calculated the crystallites size:

Table 1 Summary of different specimens.

Sample	Ti precursor	T calcination (°C)	Synthesis method	Yield (%)
NT1	TEOT	600	Microemulsion	80
NT2	TEOT	450	Microemulsion	91
NT3	TiBUT	600	Microemulsion	93
NT4	TiBUT	450	Microemulsion	88
NT5	TEOT	450	One-pot	82
NT6	TiBUT	450	One-pot	95

$$D = \frac{K \cdot \lambda}{FWHM \cdot \cos\theta}, \quad (1)$$

where D is the crystallite size; K is a dimensionless shape factor with typical values close to unity (0.94 for spherical crystallites), λ is the X-Ray wavelength (1.5418 Å), cos θ is the peak position 2θ/θ in radiant, and FWHM is the Full Width Half Maximum calculated by Origin.

Lambda 2 UV/Vis spectrometer (PerkinElmer, Canada) was used for the determination of the MB dye concentration. The UV/Vis spectrometer features double beam optics and recording the spectra over the 190–1100 nm range. A Beer–Lambert diagram was used to correlate the absorbance at 664 nm to MB concentration.

2.5. Photocatalytic activity

To evaluate the photocatalytic activity, 0.6 g L^{-1} of TiO_2 powder, calcined at different temperatures was suspended in a 50.0 mL of aqueous MB solution (2.5×10^{-5} M) in a conical flask and stirred for 30 min in dark at room temperature. Solar tests were carried out in June at 35-38 °C, with an RH of 65 % and South orientation. Simultaneously, a blank experiment without the catalyst was carried out. At regular intervals of time aliquots of 3.0 mL of MB solution were collected from the flask, centrifuged and the UV–Vis absorption spectrum of the clear solution was recorded using a double beam spectrophotometer. The decrease in the absorbance value at 664 nm wavelength, corresponding to the typical peak for the absorption spectra of MB, was utilized to determine the extent of degradation of MB and the photocatalysis activity of the sample with respect to irradiation time. The following equation was used to calculate the photodegradation rate of MB:

$$Degradation\ (\%) = \frac{(A_0 - A_t)}{A_0} \times 100\,, \quad (2)$$

where A_0 is the absorbance of initial MB, A_t is the absorbance of the solution after being irradiated for a period of t minutes. According to the first-order kinetics reaction, rate constant k (min^{-1}) was determined by using the following relation:

$$\ln\left(\frac{C_t}{C_0}\right) = -k\,t\,. \quad (3)$$

C_t was the concentration after a period of t minutes, and C_0 represented the initial concentration. The degradation process was monitored following the absorbance at the maximum UV-Vis spectrum of the target molecule (664 nm). Since the degradation pathway for the selected dye is well known [36], the eventual formation of by-products was controlled, monitoring the overall UV-Vis spectrum of the solutions recovered at different times.

3. RESULTS AND DISCUSSION

The titania nanoparticles were synthesized using a modified method reported for both one-pot synthesis [35] and microemulsion [34]. In the one-pot protocol the surfactant P123 act as a templating agent by modulating its Critical Micelle Concentration (CMC) when solubilized in water. The role of HCl is to stabilize the titanium precursor onto the templating agent, delaying its hydrolysis and condensation reaction [29], which is subsequently triggered in the hydrothermal reactor. In contrast, in the microemulsion synthesis, the surfactant and co-surfactant operate by reducing the interfacial tension between the water and oil phases. Moreover, they stabilize the microemulsion by introducing double-layer forces and/or solvation forces between dispersed particles. The hydrolysis and condensation reactions occur at 1 atm, pH 7, and 70 °C, concomitant with the urea decomposition.

The SEM analysis was carried out to evaluate the morphological structure of the nanoparticles. In Figure 1, SEM micrographs depict samples synthesized through microemulsion methods (a-d), one-pot synthesis (e,f), and P25 commercial titania nanoparticles (g) as reference material. TiO_2 nanoparticles predominantly appear as agglomerates without a characteristic shape (Figure 1 a, c, and d), resulting from the aggregation of nanostructured TiO_2 grains with an average size of approximately 30-50 nm, including the commercial titania P25. Conversely, the NT2 sample, obtained through microemulsion and calcined at low temperature (Figure 1b), seems to be composed of titania nanograins organized into spherical nanoparticles with a size of 900 nm. These spherical particles appear weakly sintered, with residual titania nanograins found on the surface of the aggregates. It is known that the calcination step, used for removing organic residues, typically enhances crystallinity but also affects the ordered mesoporous framework of TiO_2, leading to the structural collapse. This effect is evident in sample NT1 (Figure 1a), where titania nanoparticles are strongly sintered. Samples NT2, NT3, and NT4 exhibit weakly sintered TiO_2 grains, as shown in the SEM micrographs (Figure 1b-d). Notably, NT3 (Figure 2c) seems the only sample where titania nanoparticles are well-distributed, as the commercial P25 sample (Figure 1g). Samples obtained from the one-pot synthesis are characterized by a globular shape (Figure e-f), such as NT2, with an average size of about 1 μm. Such results suggest that shape and structure of TiO_2 nanograins,

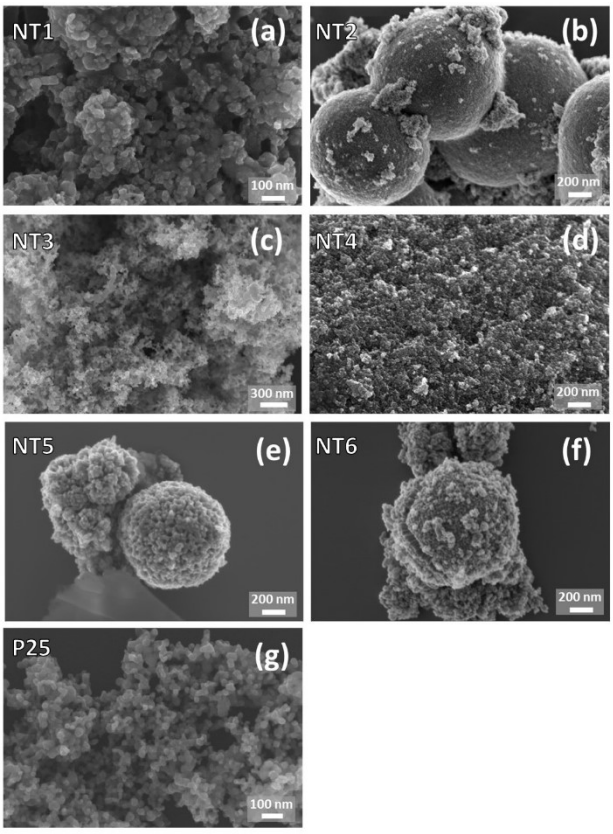

Figure 1 SEM micrographs of the samples (a) NT1, (b) NT2, (c) NT3, (d) NT4, (e) NT5, (f) NT6 and (g) P25.

obtained by using microemulsion, are strongly dependent by the alkoxide adopted as a precursor, as well as the calcination temperature. The following refluxing treatment does not influence the final shape, structure, and size of the synthesized nanoparticles. Nevertheless, in the case of one-pot synthesis, the shape of the nanoparticles seems to be influenced only by the alkoxide precursor utilized.

Phase identification of the synthesized titania nanoparticles and commercial P25 titania was carried out through XRD analysis, and the diffraction patterns are displayed in Figure 2. The XRD patterns exhibit narrower diffraction peaks when the temperature is increased from 450 to 600 °C. As depicted in Figure 2, the formation of crystallite phases begins at 450 °C, showing broad 2θ reflected peaks. When the calcination temperature is set at 600 °C, the peaks maintain the 2θ position and become narrower, indicating good crystallite formation and resulting in a white powder. The anatase phase exhibits index reflection peaks at 25.3°, 37.7°, 48.2°, 53.9°, 55.0°, and 62.0°, while rutile phase reflection peaks are observed at 27.5°, 36.1°, 41.3°, 62.8°, and 68.8° (JCPDS No. 73-1764). Both anatase and rutile phases are present in commercial P25, as well as NT1, with an average nano-crystallite size obtained by the peak reflection of anatase (101) and rutile (110) phases by the Scherrer formula, approximately 22-28 nm, and 21-52 nm, respectively. In NT2, NT3, and NT4, the 2θ reflected peaks confirm the presence of the anatase phase, with an average size of anatase crystallites about 10-25 nm. Conversely, samples NT5 and NT6 showed peaks of the rutile phase with an initial formation of anatase crystallites with an average size of rutile crystallites about 8-12 nm. XRD data confirm the important role played by the choice of titanium precursor and the calcination temperature for the microemulsion synthesis. In fact, the use of TEOT leads to the formation of mixed anatase and rutile phases, whereas TiBUT to the anatase phase. On the other hand, diffraction patterns for the samples coming from one-pot synthesis demonstrate that the change of titanium alkoxide does not influence the polymorphic phase, mainly constituted by the rutile phase.

Spectroscopic and kinetic studies on the degradation of MB were carried out under solar irradiation, and the photocatalytic activity was compared to commercial P25 titania nano powder. A solution of MB and synthesized titania nanoparticles was exposed to solar irradiation for 60 minutes. The initial concentration of MB was 2.5×10^{-5} M, and the catalyst dosage was 0.6 g L^{-1}. UV-Vis spectra of the irradiated solution were recorded and monitored in the range of 400–700 nm at different photoreaction times (15, 30, 45, and 60 minutes). Figure 3 displays the degradation rate (D%) of MB adsorption as a function of the time. The photocatalytic degradation of a MB solution by NT2, NT4, and P25 photocatalysts exhibit a photodegradation rate of approximately 90 % after 60 minutes. In contrast, the degradation rate of MB is around 52 % for NT1, 40 % for samples NT3 and NT5, and 30 % for sample NT6. The good photocatalytic activity of NT2 and NT4 is probably due to the larger presence of anatase crystallites compared to NT5 and NT6, mainly populated by rutile crystallites. The high photoreactivity of anatase is indeed well reported in literature [37]. The calculated kinetic parameters of MB degradation in samples NT2, NT4, and P25 have the highest reaction rate constant of about 1.8×10^{-2} min^{-1}, indicating excellent photocatalytic activity. Conversely, NT1, NT3, NT5, and NT6 show a low-rate constant of about 2.7×10^{-3}, 1.7×10^{-3}, 7.5×10^{-3}, and 5.1×10^{-3}, respectively. Photocatalytic activity is significantly higher in samples NT2 and NT4, improving by one order of magnitude from 2.7×10^{-3} min^{-1} to 1.7×10^{-2} min^{-1} and from 1.7×10^{-3} min^{-1} to 1.7×10^{-2} min^{-1}, respectively only by changing the calcination temperature.

Among the samples synthetized through microemulsion, an improvement in the photocatalytic activity was achieved decreasing the calcination temperature to 450 °C. To comprehensively understand how calcination temperature influences photocatalytic activity, additional experiments are necessary to explore the geometry of anatase TiO_2 single crystals and their textural properties using alternative techniques such as N_2 physisorption and TEM. As highlighted by Zhang [38], it is

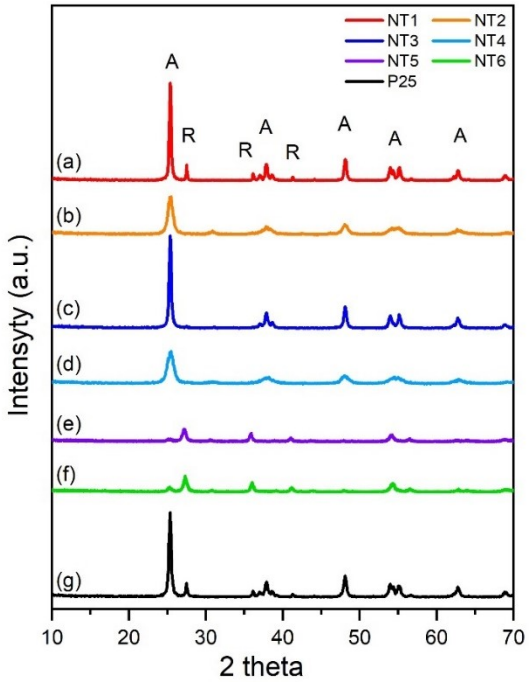

Figure 2 XRD spectra of the samples (a) NT1, (b) NT2, (c) NT3, (d) NT4, (e) NT5, (f) NT6, and (g) P25.

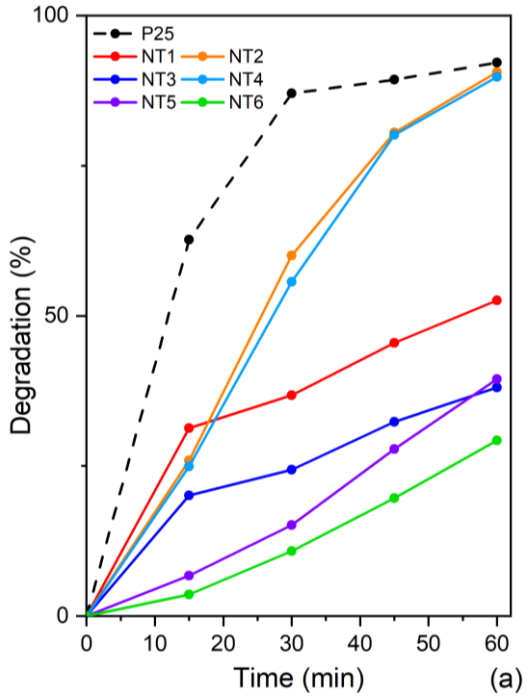

Figure 3 MB degradation under solar irradiation.

feasible to enhance the degradation rate of a methyl orange solution to 93.6 % after 60 minutes using doped titania (Ag-TiO_2). This material is characterized by the (001) crystal plane of anatase with an exposure ratio of 41.8 %. In anatase phase TiO_2, the (001) plane corresponds to the high-energy crystal surface, while the (101) plane is associated with the stable crystal surface. Consequently, the (001) crystal surface has high energy and good reactivity. In photocatalytic reactions, photogenerated electrons transfer and accumulate on the (101) crystal planes of lower energy. Conversely, photogenerated holes tend to accumulate on (001) crystal planes with high energy. This distinctive feature effectively promotes the separation of photogenerated electron-hole pairs, thereby enhancing photocatalytic performance.

These preliminary results suggest that the crystallite phase and textural properties play a fundamental role in photocatalytic activity. On the one hand, samples obtained through microemulsion method and calcined at low temperatures are predominantly composed of anatase and show catalytic activity comparable to commercial P25. Moreover, the lower calcination temperature could change the textural properties increasing their surface area. On the other hand, samples obtained using the one-pot method and calcined at low temperatures show the presence of the only rutile phase. Changes in the crystallite phase may be due to the role played by the HCl. In fact, it is reported in literature that HCl may induce a phase transition from anatase to rutile as a function of the acid concentration [39].

Moreover, XRD peak intensities for such synthesis products are much lower than those obtained from the analysis of samples coming from the microemulsion approach. This suggests the not well formation of crystallites that may reasonably imply a small exposure of 001 crystal planes, thus influencing photocatalytic activity.

4. CONCLUSION

Commercial titania nanoparticles are demonstrated having great capabilities to degrade environmental pollutants; however, its use in the architectural field is still not largely diffused due to the high costs and the environmental impact related to the industrial production. A low-cost and environmentally friendly synthesis is therefore required to increase the adoption of such material in the formulation of paint, mortar, and protective coatings. In this work, nanostructured TiO_2 was synthesized using two distinct approaches: microemulsion and a one-pot route, both resulting in high synthesis yields. This study aims to identify the most efficient synthesis route for producing titania nanoparticles by utilizing a solvent-free procedure. In the water-in-oil (W/O) microemulsion was employed a volume ratio of 1:1, intending to reduce the oil volume content typically found in the literature. Additionally, a solvent-free synthesis in an acidic environment was conducted, employing an alkoxide precursor and a triblock polymer surfactant. The synthesis procedures were conducted under atmospheric pressure, obtaining high synthesis yield (82-95 %). All these parameters align with the principles of green chemistry and sustainability. The resulting samples were obtained as white powders with high crystallinity and purity. Structural, compositional, and morphological characterizations were carried out on the samples. Among the synthesized samples, NT2 exhibited an attractive shape and superior photoactivity compared to the widely used P25 commercial nanoparticles. The outstanding photocatalytic performances were attributed to the exposed crystal plane and morphological properties achieved by adjusting the calcination temperature.

ACKNOWLEDGEMENT

The authors would like to thank the late Dr. Igor Luisetto for his considerable help, inspiration, that made this work possible. The authors would like to thank Fondazione Roma (Grant No. 5229441F37) and Regione Lazio under ERCOLE (CUP F 85 F 21001090003) and GRAL project (CUP F 85 F 21001710009) for research funding. The authors also acknowledge funding from the European Union - NextGenerationEU- CHANGES – CUP B83C22005060006 Project code: PE00000020, "Istruzione e ricerca"-Componente 2 "Dalla ricerca all'impresa"-Investimento 1.3, Partenariato Esteso 5 through the Excellence Centre at the Lazio Technological District for Cultural Heritage (DTC Lazio). LT also acknowledges Ministry of Education, Universities and Research FINANZIAMENTO DIPARTIMENTI DI ECCELLENZA 2023 2027 (Art 1 commi 314 337 Legge 11 12 2016 n 232 project.

REFERENCES

[1] F. Bartoli, L. Corradi, Z. Hosseini, A. Privitera, M. Zuena, A. Kumbaric; V. Graziani, L. Tortora, A. Sodo, G. Caneva, In Vitro Viability Tests of New Ecofriendly Nanosystems Incorporating Essential Oils for Long-Lasting Conservation of Stone Artworks, Gels, 2024, 10, 132.
DOI: 10.3390/gels10020132

[2] F. Bartoli, Z. Hosseini; V. Graziani, M. Zuena, C. Venettacci, G. Della Ventura, L. Tortora, A Sodo, G Caneva, In Situ Evaluation of New Silica Nanosystems as Long-Lasting Methods to Prevent Stone Monument Biodeterioration, Coatings 2024, 14, 163.
DOI: 10.3390/coatings14020163

[3] S. Yasmeen, L. Burratti, L. Duranti, E. Sgreccia, P. Prosposito, Photocatalytic Degradation of Organic Pollutants - Nile Blue, Methylene Blue, and Bentazon Herbicide—Using NiO-ZnO Nanocomposite, Nanomaterials 2024, 14, 470.
DOI: 10.3390/nano14050470

[4] E. Marconi; I. Luisetto; G. Di Carlo; M. P. Staccioli; S. Tuti; L. Tortora, 3-APTES on Dendritic Fibrous Mesoporous Silica Nanoparticles for the pH-Controlled Release of Corrosion Inhibitors, Nanomaterials 2023, 13, 2543.
DOI: 10.3390/nano13182543

[5] S. W. Lam, A Soetanto, R. Amal, Self-cleaning performance of polycarbonate surfaces coated with titania nanoparticles, J Nanopart Res 11 (2009), pp. 1971–1979.
DOI: 10.1007/s11051-008-9555-0

[6] D. Camuffo, M. Del Monte, C. Sabbioni, Origin and growth mechanisms of the sulfated crust on urban limestone, vol. 19, no. c, 1983, pp. 351–359.
DOI: 10.1007/BF00159596

[7] E. Franzoni, A. Fregni, R. Gabrielli, G. Graziani, E. Sassoni, Compatibility of photocatalytic TiO2-based finishing for renders in architectural restoration: A preliminary study, Build Environ, vol. 80, 2014, pp. 125–135.
DOI: 10.1016/j.buildenv.2014.05.027

[8] K. Hashimoto, H. Irie, A. Fujishima, TiO 2 photocatalysis: A historical overview and future prospects, Japanese Journal of Applied Physics, Part 1: Regular Papers and Short Notes and Review Papers, vol. 44, no. 12, 2005, pp. 8269–8285.
DOI: 10.1143/JJAP.44.8269

[9] T. Maggos, J. G. Bartzis, M. Liakou, C. Gobin, Photocatalytic degradation of NOx gases using TiO2-containing paint: A real scale study, J Hazard Mater, vol. 146, no. 3, 2007, pp. 668–673.
DOI: 10.1016/j.jhazmat.2007.04.079

[10] A. M. Ramirez, K. Demeestere, N. De Belie, T. Mäntylä, E. Levänen, Titanium dioxide coated cementitious materials for air purifying purposes: Preparation, characterization and toluene removal potential, Build Environ, vol. 45, no. 4, 2010, pp. 832–838.
DOI: 10.1016/j.buildenv.2009.09.003

[11] H. Babaizadeh, M. Hassan, Life cycle assessment of nano-sized titanium dioxide coating on residential windows, Constr Build Mater, vol. 40, 2013, pp. 314–321.
DOI: 10.1016/j.conbuildmat.2012.09.083

[12] N. T. Padmanabhan, H. John, Titanium dioxide based self-cleaning smart surfaces: A short review, J Environ Chem Eng, vol. 8, no. 5, 2020, p. 104211.
DOI: 10.1016/j.jece.2020.104211

[13] L. Ruggiero. M. R. Fidanza, M. Iorio (+ another 4 authors) , Synthesis and Characterization of TEOS Coating Added With Innovative Antifouling Silica Nanocontainers and TiO2 Nanoparticles, Front Mater, vol. 7, no. June, 2020.
DOI: 10.3389/fmats.2020.00185

[14] L. Tortora, G. Di Carlo, M. Moquera, G. Ingo, Editorial: Nanoscience and Nanomaterials for the Knowledge and Conservation of Cultural Heritage, Frontiers in Materials, vol. 7, 2020.
DOI: 10.3389/fmats.2020.606076

[15] L. Pinho, M. J. Mosquera, Titania-silica nanocomposite photocatalysts with application in stone self-cleaning, Journal of Physical Chemistry C, vol. 115, no. 46, 2011, pp. 22851–22862.
DOI: 10.1021/jp2074623

[16] L. A. M. Carrascosa, R. Zarzuela, N. Badreldin, M. J. Mosquera, A Simple, Long-Lasting Treatment for Concrete by Combining Hydrophobic Performance with a Photoinduced Superhydrophilic Surface for Easy Removal of Oil Pollutants, ACS Appl Mater Interfaces, vol. 12, no. 17, 2020, pp. 19974–19987.
DOI: 10.1021/acsami.0c03576

[17] M. Hussain, N. Russo, G. Saracco, Photocatalytic abatement of VOCs by novel optimized TiO2 nanoparticles, Chemical Engineering Journal, vol. 166, pp 138-149, 2011,
DOI: 10.1016/j.cej.2010.10.040

[18] D. S. Bhatkhande, V. G. Pangarkar, A. C. M. Beenackers, Photocatalytic degradation for environmental applications – a review, Journal of Chemical Technology & Biotechnology: International Research in Process, Environmental & Clean Technology 77.1 (2002): pp. 102-116.
DOI: 10.1002/jctb.532

[19] M. J. Gázquez, J. P. Bolívar, R. Garcia-Tenorio, and F. Vaca, "A Review of the Production Cycle of Titanium Dioxide Pigment," Materials Sciences and Applications, vol. 05, no. 07, pp. 441–458, 2014,
DOI: 10.4236/msa.2014.57048

[20] J. Jing, Y. Guo, S. Wang, F. Chen, L. Yang, G. Qiu, Recent Progress in Electric Furnace Titanium Slag Processing and Utilization: A Review, Crystals (Basel), vol. 12, no. 7, 2022.
DOI: 10.3390/cryst12070958

[21] M. A. Irshad, R. Nawaz, M. Zia ur Rehman (+ another 5 authors), Synthesis, characterization and advanced sustainable applications of titanium dioxide nanoparticles: A review, Ecotoxicol Environ Saf, vol. 212, 2021, p. 111978.
DOI: 10.1016/j.ecoenv.2021.111978

[22] P. Nyamukamba, O. Okoh, H. Mungondori, R. Taziwa, S. Zinya, "Synthetic Methods for Titanium Dioxide Nanoparticles: A Review," Titanium Dioxide - Material for a Sustainable Environment, 2018,
DOI: 10.5772/intechopen.75425

[23] S. Sagadevan, S. Imteyaz, B. Murugan, J. A. Lett, N. Sridewi, G. K. Weldegebrie, I. Fatimah, W. Oh, A comprehensive review on green synthesis of titanium dioxide nanoparticles and their diverse biomedical applications, Green Processing and Synthesis, vol. 11, no. 1, 2022, pp. 44-63.
DOI: 10.1515/gps-2022-0005

[24] F. Wu, Z. Zhou, A. L. Hicks, Life Cycle Impact of Titanium Dioxide Nanoparticle Synthesis through Physical, Chemical, and Biological Routes, Environ Sci Technol, vol. 53, no. 8, 2019, pp. 4078–4087.
DOI: 10.1021/acs.est.8b06800

[25] E. Grabowska, M. Marchelek, M. Paszkiewicz-Gawron, A. Zaleska-Medynska, Metal oxide photocatalysts. Elsevier Inc., 2018.
DOI: 10.1016/B978-0-12-811634-0.00003-2

[26] K. Lan. R. Wang, Q. Wei (+ another 4 authors), Stable Ti 3+ Defects in Oriented Mesoporous Titania Frameworks for Efficient Photocatalysis, Angewandte Chemie, vol. 132, no. 40, 2020, pp. 17829–17836.
DOI: 10.1002/ange.202007859

[27] E. M. Samsudin, S. B. A. Hamid, J. C. Juan, W. J. Basirun, Influence of triblock copolymer (pluronic F127) on enhancing the physico-chemical properties and photocatalytic response of mesoporous TiO 2, Appl Surf Sci, vol. 355, 2015, pp. 959–968.
DOI: 10.1016/j.apsusc.2015.07.178

[28] R. Zhang, A. A. Elzatahry, S. S. Al-Deyab, D. Zhao, Mesoporous titania: From synthesis to application, Nano Today, vol. 7, no. 4, 2012, pp. 344–366.
DOI: 10.1016/j.nantod.2012.06.012

[29] B. Bonelli, S. Esposito, F. S. Freyria, Mesoporous Titania: Synthesis, Properties and Comparison with Non-Porous Titania, Titanium Dioxide, 2017.
DOI: 10.5772/intechopen.68884

[30] A. M. Luís, M. C. Neves, M. H. Mendonça, O. C. Monteiro, Influence of calcination parameters on the TiO2 photocatalytic properties, Mater Chem Phys, vol. 125, no. 1–2, 2011, pp. 20–25.
DOI: 10.1016/j.matchemphys.2010.08.019

[31] M. Andersson, L. Österlund, S. Ljungström, A. Palmqvist, Preparation of nanosize anatase and rutile TiO2 by hydrothermal treatment of microemulsions and their activity for photocatalytic wet oxidation of phenol, Journal of Physical Chemistry B, vol. 106, no. 41, 2002, pp. 10674–10679.
DOI: 10.1021/jp025715y

[32] M. Fernández-García, X. Wang, C. Belver, J. C. Hanson, J. A. Rodriguez, Anatase-TiO2 Nanomaterials: Morphological/Size Dependence of the Crystallization and Phase Behavior Phenomena, J. Phys. Chem. C 2007, 111, 2, pp. 674–682,
DOI: 10.1021/jp065661i

[33] C.-H. Lu, M.-C. Wen, Synthesis of nanosized TiO2 powders via a hydrothermal microemulsion process, Journal of Alloys and Compounds Vol. 448, Issues 1–2, 2008, pp 153-158.
DOI: 10.1016/j.jallcom.2007.01.043

[34] E. Marconi, L. Tortora "Synthesis of titania nanoparticles in W/O microemulsion: moving the production toward a green approach" IMEKO TC4 Int. Conf. on Metrology for Archaeology and Cultural Heritage, 2023
DOI: 10.21014/tc4-ARC-2023.091

[35] C. Lin, K. Tao, H. Yu, D. Hua, S. Zhou, Enhanced catalytic performance of molybdenum-doped mesoporous SBA-15 for metathesis of 1-butene and ethene to propene, Catal. Sci. Technol., 2014, 4, pp. 4010-4019,
DOI: 10.1039/C4CY00652F

[36] A. Houas, H. Lachheb, M. Ksibi, E. Elaloui, C. Guillard, J. M. Herrmann, Photocatalytic degradation pathway of methylene blue in water, Appl Catal B, vol. 31, no. 2, 2001, pp. 145–157.
DOI: 10.1016/S0926-3373(00)00276-9

[37] M. Buchalska, M. Kobielusz, A. Matuszek, M. Pacia, S. Wojtyła, W. Macyk, On Oxygen Activation at Rutile- and Anatase-TiO_2, ACS Catalysis 2015 5 (12), pp. 7424-7431.
DOI: 10.1021/acscatal.5b01562

[38] L.-Y. Zhang, J. You, Q.-W. Li (+ another 4 authors) , Preparation and Photocatalytic Property of Ag Modified Titanium Dioxide Exposed High Energy Crystal Plane (001), vol. 10, no. 27, 2020.
DOI: 10.3390/coatings10010027

[39] K. Lan, R. Wang, W. Zhang (+ another 7 authors), Mesoporous TiO_2 microspheres with precisely controlled crystallites and architectures, Chem 4.10 (2018): pp. 2436-2450.
DOI: 10.1016/j.chempr.2018.08.008